# Thiocyanato complexes of the coinage metals: synthesis and crystal structures of the polymeric pyridine complexes [Ag$_x$Cu$_y$(SCN)$_{x+y}$(py)$_z$]

Harald Krautscheid,* Norbert Emig, Nicole Klaassen and Petra Seringer

*Institut für Anorganische Chemie, Universität Karlsruhe (TH), D-76128 Karlsruhe, Germany*

From solutions of CuSCN or AgSCN in pyridine, several pyridine complexes of the thiocyanates with varying compositions and crystal structures were isolated depending on the reaction conditions. In CuSCN and in the orthorhombic modification of AgSCN the SCN$^-$ anions co-ordinate to four metal atoms as 1,1,1,3-$\mu_4$ bridges, whereas the degree of bridging decreases with increasing amounts of pyridine in the polymeric complexes [Cu(SCN)(py)$_z$] and [Ag(SCN)(py)$_z$] ($z = 1$ or 2). The distorted tetrahedral co-ordination of the metal atoms is preserved by co-ordination of pyridine ligands. Especially in the heteronuclear complexes [AgCu(SCN)$_2$(py)$_4$], [AgCu(SCN)$_2$(py)$_3$] and [Ag$_2$Cu(SCN)$_3$(py)$_3$], interesting variants of structures result from the different possible modes of co-ordination of the SCN$^-$ ligand and from the preferred co-ordination of the "soft" S atoms to the "soft" Ag$^+$ ions as defined by Pearson's hard and soft acid and base principle.

In the course of our investigations of the synthesis and structure of polynuclear and polymeric halogeno and pseudo-halogeno complexes[1] we are now examining thiocyanato complexes of the coinage metals. With its ambidexterous character the SCN$^-$ anion is expected to show a rich variety of co-ordination modes, which is already expressed by the 1,1,1,3-$\mu_4$ bridging mode in CuSCN: in both CuSCN modifications each N atom binds to one and each S atom binds to three Cu atoms,[2,3] by which the copper centers are co-ordinated in a distorted tetrahedral fashion. Numerous SCN$^-$ complexes of the transition metals are known.[4–6] According to Pearson's principle[7] of hard and soft Lewis acids and bases (HSAB) the elements of the first transition series act as "hard" Lewis acids and form mainly thiocyanato-$N$ complexes ("isothiocyanate"), the electron rich metals of the 4d and 5d elements usually form thiocyanato-$S$ complexes ("thiocyanate"). For some metals the type of co-ordination, M–SCN or M–NCS, is determined by the other ligands bound and by steric interactions.[8]

The formation and crystal structures of complexes of CuSCN and AgSCN with various donor ligands like substituted pyridine ligands have been reported by White and co-workers.[9–11] In these compounds the solid state structure is considerably influenced by the steric properties of the ligands. For example, the large 2,6-dimethylpyridine ligand and AgSCN form polymeric chains of [Ag(SCN)(2,6-Me$_2$py)] with approximately trigonal planar co-ordinated Ag atoms. With quinoline [Ag(SCN)(quin)$_2$] chains are formed, while 2-methyl- or 3-methyl-pyridine and AgSCN yield different polymeric layer structures.[10] Apart from this type of compound only few anionic, homoleptic thiocyanato complexes of Ag$^+$ and Cu$^+$ are known, for example [C$_6$H$_8$N][Ag(SCN)$_2$], [Hpy][Cu$_2$(SCN)$_3$], or the tetrathiofulvalene derivative [ttf][Cu(SCN)$_2$].[12] In the iodo-thiocyanatometalates [NEt$_4$]$_2$[M$_4$I$_4$(SCN)$_2$] (M = Ag or Cu), M$_4$I$_4$ heterocubane fragments are linked by 1,3-$\mu$-bridging SCN$^-$ ligands to form two- and three-dimensional polymeric structures.[13] The MS$_4^{2-}$ (M = Mo or W) anions have been utilized to combine (CuSCN)$_n$ units to infinite chains and networks, *e.g.* in [NEt$_4$]$_2$[{Cu(NCS)}$_3$WS$_4$] or [PPh$_4$]$_2$[{Cu(NCS)}$_4$WS$_4$].[14]

We are now investigating the influence of synthesis and crystallization conditions on the solid-state structures of copper and silver thiocyanato complexes with unsubstituted pyridine ligands. Further we report on the co-ordination modes of SCN$^-$ ligands in neutral and heteronuclear Cu$^+$/Ag$^+$ pyridine complexes with bridging thiocyanate.

## Results and discussion

Whereas CuSCN is of low solubility or insoluble in almost all organic solvents, it is soluble in pyridine forming a greenish yellow solution. Slow condensation of diethyl ether into a solution of CuSCN in pyridine leads to the formation of colorless, monoclinic crystals of [Cu(SCN)(py)] **1** mostly growing in large clusters. However, yellow-green rods of [Cu(SCN)(py)$_2$] **2** are formed by slow evaporation of the solvent from the pyridine solution. The IR data of **1** have been assigned to bridging SCN$^-$ ions in various publications, but no statement about the exact co-ordination has been made.[15] Colorless platelets of [Ag(SCN)(py)] **3** are formed by slow evaporation of the solvent as well as by layering a solution of AgSCN in pyridine with diethyl ether at room temperature. The pyridine rich complex [Ag(SCN)(py)$_2$] **4** crystallizes as small colorless rods and is only stable in pyridine at low temperatures; at room temperature **4** decomposes by liberation of pyridine within a few seconds.

Layering a pyridine solution of CuSCN and AgSCN with diethyl ether at $-30\,°C$ yields yellow crystals of [AgCu-(SCN)$_2$(py)$_4$] **5**. Adding only small amounts of diethyl ether to a solution of CuSCN and AgSCN at room temperature or slow evaporation of the solvent *in vacuo* leads to the formation of crystals of [AgCu(SCN)$_2$(py)$_3$] **6** as yellow platelets. When separated from the mother-liquor **5** and **6** are unstable and decompose losing pyridine. Also, warming up crystalline **5** in the mother-liquor, or addition of extra ether to crystals of **5** or **6** in pyridine–ether, leads to dissolution of the primary products and formation of light yellow, prismatic crystals of [Ag$_2$Cu(SCN)$_3$(py)$_3$] **7**. Compound **7** is air stable at room temperature.

We were able to perform crystal structure analyses of compounds **1**–**7**. Selected bond lengths and angles are given in the captions below the figures.

Fig. 1(b) shows the result of the crystal structure analysis of [Cu(SCN)(py)] **1** (space group *Cc*). Each Cu atom is bound to two S atoms and one N atom of three thiocyanate ligands. Two Cu atoms are bridged almost symmetrically by the S atom of
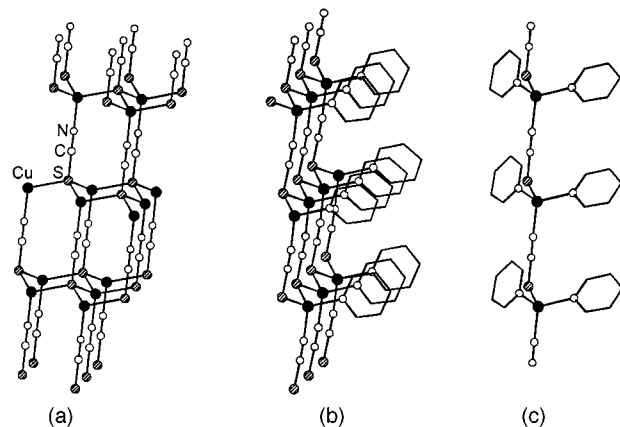
**Fig. 1** Co-ordination of the Cu atoms by bridging thiocyanate ligands in β-CuSCN,[2] compounds **1** and **2**: (a) fragment of the crystal structure of β-CuSCN;[2] Cu–S 234.3(1), Cu–N 192(1), C–N 115(2), C–S 168.3(9) pm; (b) fragment of the crystal structure of **1**, view along a Cu–SCN layer perpendicular to the [1 0 0] direction; Cu–S 235.8, 237.7(2), Cu–N 195.7(5), Cu–N (py) 205.4(5), C–N 115.6(8), C–S 166.0(6) pm; (c) fragment of the one-dimensional infinite structure of **2**; Cu–S 230.4(1), Cu–N 195.2(2), Cu–N (py) 206.5, 210.3(2), C–N 115.6(3), C–S 165.6(3) pm.

the 1,1,3-$\mu_3$-SCN ligands [Cu1–S1 235.8(2); Cu1–S1′ 237.7(2) pm]. The fourth co-ordination site is occupied by a pyridine ligand. With bond angles between 105.9(1) and 111.4(1)° the Cu atoms are co-ordinated approximately in a tetrahedral fashion; the SCN⁻ groups are linear [S1–C1–N1 178.1(5)°]. Ten-membered rings consisting of three Cu atoms, two thiocyanate ligands and one S atom of an additional SCN⁻ group are recognizable as a typical fragment of **1**. These rings in chair conformation share common edges to form a two-dimensional, infinite network, similar to that of the linked six-membered rings in grey arsenic. The stacking of these layers along the [1 0 0] direction leads to a polar structure, since the SCN⁻ groups are aligned in the same direction and the pyridine ligands have the same orientation in all layers. In contrast to **1**, the methylpyridine derivatives [Cu(SCN)(2,6-Me₂py)] and [Cu(SCN)(2-Mepy)] crystallize as polymeric chains with co-ordination number 3 for the Cu atoms and polymeric double chains, respectively.[11]

According to the crystal structure analysis [Cu(SCN)(py)₂] **2** (space group $P2_1/n$) consists of infinite chains arranged parallel to the crystallographic *a* axis. Fig. 1(c) shows that the thiocyanate anions act as 1,3-μ bridging ligands. Each Cu atom is co-ordinated by one sulfur atom of an SCN⁻ ligand, one nitrogen atom of another SCN⁻ ligand, and by two pyridine ligands. So the Cu⁺ ion is located in a slightly distorted tetrahedral ligand field. The N–Cu–N and N–Cu–S bond angles range from 101.3(1) to 112.3(1)°; the thiocyanate ligand is almost linear [S1–C1–N1 178.4(3)°]. The Cu–N bond lengths to the pyridine ligands [206.5(2) and 210.3(2) pm] are significantly longer than to the SCN⁻ anion [Cu1–N1 195.2(2); Cu1–S1 230.4(1) pm]. The crystal structure of **2** corresponds well to those observed for [Cu(SCN)(3-Mepy)₂] and [Cu(SCN)(4-Mepy)₂], but the parallel arrangement of the thiocyanate groups is in marked contrast to that of [Cu(SCN)(2-Mepy)₂].[11]

In the 3R polytype of the β modification of CuSCN[2] the Cu atoms are co-ordinated by a fourth thiocyanate group through the S atom instead of the pyridine molecule as in **1**. This leads to a three-dimensional network [Fig. 1(a)], where the thiocyanate ligands are 1,1,1,3-$\mu_4$ bridging. The C–N bond lengths as well as the S–C–N angles are insensitive towards the bridging mode, whereas the C–S bond lengths become longer and the Cu–N bond lengths shorter with a higher degree of bridging. Fig. 1 illustrates the relationship of compounds **1** and **2** with β-CuSCN regarding the linkage of the Cu atoms by the thiocyanate ligands. The step-by-step insertion of pyridine ligands

**Table 1** Raman data (SCN⁻ vibrations) of β-CuSCN, **1**, **2**, **3** and **7**

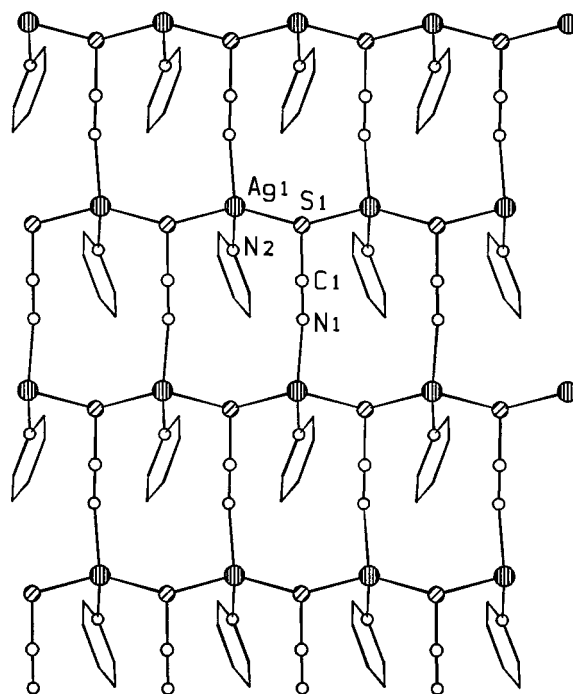|  | β-CuSCN | **1** | **2** | **3** | **7** |
|---|---|---|---|---|---|
| $\tilde{\nu}_{C-N}$/cm⁻¹ | 2170 | 2120 | 2099 | 2116 | 2133 |
| $\tilde{\nu}_{C-S}$/cm⁻¹ | 746 | 754 | 767 | 745 | 751 |
| $\delta_{S-C-N}$/cm⁻¹ | 433 | 448 | 463 |  | 448 |



**Fig. 2** Fragment of the network of compound **3**. View along [0 0 1] on several unit cells. Selected bond lengths: Ag–S 258.2, 260.8(3), Ag–N 223.0(5), Ag–N (py) 231.3(4), C–N 115.2(7), C–S 166.0(6) pm.

into the structure of β-CuSCN leads to a stepwise reduction of the dimensionality. Opening the three-dimensional structure of β-CuSCN in one direction leads to the formation of the two-dimensional network of compound **1**. Further insertion of pyridine finally affords the one-dimensional chain structure of **2**.

The Raman spectra of compounds **1** and **2** (Table 1) show an intense signal at $\nu_{C-N}$ 2120 and 2099 cm⁻¹, assigned to the pseudo-antisymmetric S–C–N stretching mode ("C–N stretch"). Compared with β-CuSCN ($\nu_{C-N}$ 2170 cm⁻¹),[2,15] the absorption is shifted to significantly lower wavenumbers indicating a lesser degree of bridging by the S atoms of the thiocyanate ligands in **1** and **2**. This is in agreement with infrared data reported previously.[5,15,16] At the same time the positions of the pseudo-symmetric S–C–N stretching mode $\nu_{C-S}$ ("C–S stretch") increase by 8 and 21 cm⁻¹, respectively, and the energy of the S–C–N deformation mode $\delta_{S-C-N}$ increases by 15 and 30 cm⁻¹, respectively. This shift of the S–C–N wavenumbers of **1** and **2** indicates a slightly increasing C–S bond order together with a decreasing C–N bond order with respect to β-CuSCN.

The homologous silver complex [Ag(SCN)(py)] **3** (space group $P2_12_12_1$) features, like **1**, a two-dimensional structure (Fig. 2). Again ten-membered rings are formed by two thiocyanate groups, three silver atoms and one sulfur atom. In contrast to **1**, the rings in **3** possess the boat conformation. The silver atoms have distorted tetrahedral co-ordination geometry; within each layer the SCN⁻ groups are approximately parallel. The pyridine ligands are arranged in rows and point alternately in opposite directions. Thus the Ag(SCN)(py) nets in **3** are analogous to those in [Ag(SCN)(2-Mepy)] (space group $Pna2_1$).[10] However, the structures differ in the stacking of these layers.
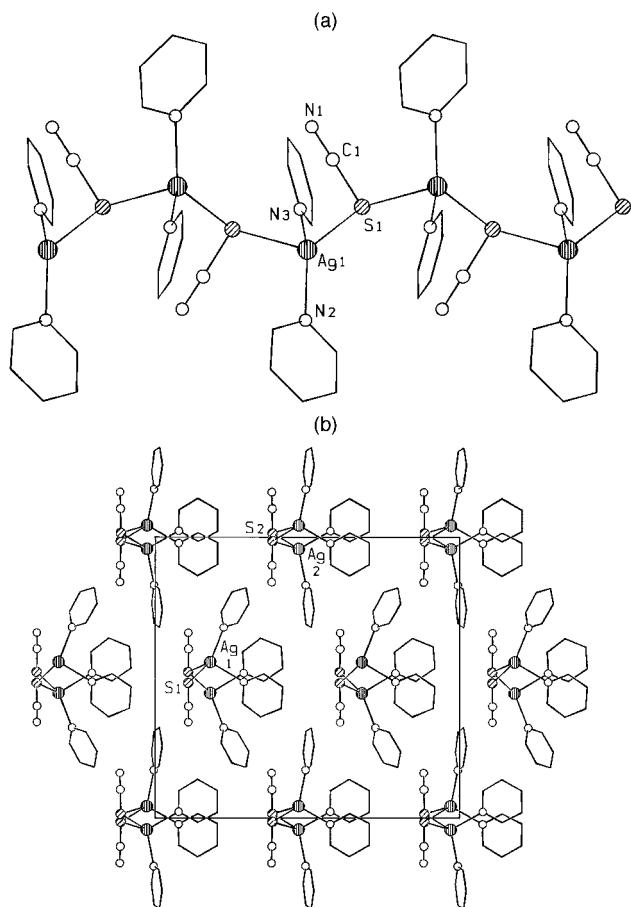
**Fig. 3** Crystal structure of compound **4**: (a) fragment of one out of two crystallographically independent polymeric chains; selected bond lengths [in square brackets for second chain]: Ag–S 252.5, 263.9(1) [248.4, 275.8(1)], Ag–N (py) 226.2, 239.7(4) [230.8, 231.5(3)], C–N 116.1(6) [115.4(6)], C–S 166.2(4) [166.7(4)] pm; (b) packing of the chains in the unit cell viewed along [1 0 0].



**Fig. 4** Fragment of the polymeric structure of compound **5**; selected bond lengths (pm) and angles (°): Ag–S1 258.21(7), Ag–S2 250.66(8), Ag–N2′ 232.6(2), Ag–N3 235.2(2), Cu–N1 193.2(2), Cu–N4 205.4(2), S1–C1 165.0(3), C1–N1 115.0(3), S2–C2 164.8(3) and C2–N2 115.1(3); S1–Ag–S2 115.87(3), S1–Ag–N2′ 99.03(6), S1–Ag–N3 103.14(6), S2–Ag–N2′ 119.55(6), N1–Cu–N4 116.2(1), Ag–S1–C1 100.24(9), Ag–S2–C2 100.31(9), Ag″–N2–C2 177.8(2), Cu–N1–C1 167.9(2), S1–C1–N1 178.3(2) and S2–C2–N2 178.5(2).

In [Ag(SCN)(py)$_2$] **4** (space group *Pca*2$_1$) the SCN$^-$ ligands act as 1,1-μ bridges and link two Ag(py)$_2$ fragments to form polymeric chains (Fig. 3). These chains expand parallel to the crystallographic *a* axis, whereby two crystallographically independent chains differing in the orientation of the pyridine rings and also in some bond lengths and angles are present. Again, the Ag atoms are co-ordinated in a distorted tetrahedral fashion [96.41–134.06(9)°]; the Ag–S bond lengths vary from 248.4 to 275.8(1) pm. The average Ag–S bond length (260.1 pm) is similar to those in **3** and in the methylpyridine complexes [Ag(SCN)(2-Mepy)] and [Ag(SCN)(3-Mepy)],[10] in which the S atoms also co-ordinate to two Ag atoms. The C–S and N–C distances as well as the S–C–N bond angles in the SCN$^-$ units are equal within the accuracy of the data. In contrast to compound **2**, in which the 1,3-μ-SCN$^-$ ligands link two Cu atoms by co-ordination through the N and S atoms, the 1,1-μ-SCN$^-$ ligands in **4** co-ordinate to the Ag atoms through sulfur alone. This co-ordination corresponds to the HSAB principle, according to which the "soft" Ag$^+$ ions should bind preferentially to the "softer" S atoms of the thiocyanate groups.

Within the Ag(SCN)(py)$_2$ chains the SCN$^-$ ligands are located in a coplanar arrangement. Fig. 3(b) shows that all Ag(SCN)(py)$_2$ chains in the unit cell of compound **4** have the same orientation, thus forming a polar structure. The alternating orientation of the SCN$^-$ groups in **4** is different from that in **3**, but it is similar to the AgSCN chains observed in the layer structure of [Ag(SCN)(3-Mepy)].[10]

In [AgCu(SCN)$_2$(py)$_4$] **5** (space group *P*2$_1$/*n*) the silver atoms are linked by 1,3-μ-bridging thiocyanate ligands to form infinite chains along the 2$_1$ screw axis (Fig. 4). A further SCN$^-$ group
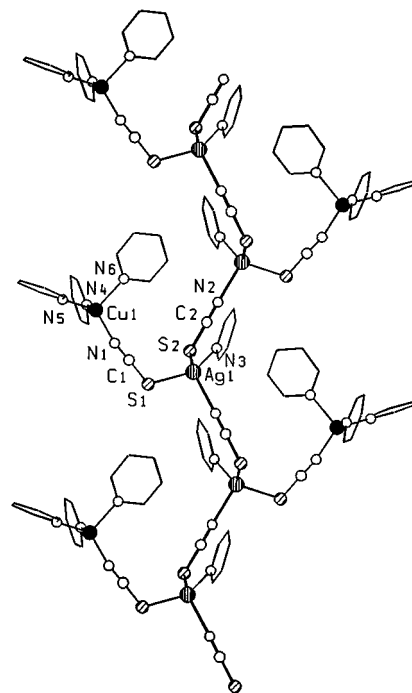
links each Ag atom of this chain to a terminal Cu(py)$_3$ unit. The fourth coordination site of silver is occupied by a pyridine molecule. The bond angle at the Ag atoms between the thiocyanate groups of the chain is 119.55(6)° (S2–Ag1–N2′). The angles S2–Ag1–S1 and S2–Ag1–N3 are 115.87(3) and 118.22(6)°, respectively, 6–10° wider than the ideal tetrahedral angle. Accordingly, the angles N2′–Ag1–S1 and N2′–Ag1–N3 are reduced to 99.03(6) and 97.58(8)°. The copper atoms are co-ordinated by the four N atoms of three pyridine molecules and the thiocyanate ligand in a distorted tetrahedral fashion [102.53(9) to 117.98(9)°].

The AgSCN backbone in compound **5** is similar to that found in the crystal structure of monoclinic AgSCN.[17] Therein the 1,3-μ-SCN$^-$ ions link the Ag atoms to form infinite chains (Ag–S 242.8, Ag–N 222.3 pm; S–Ag–N 167.2°). These chains are arranged in such a way that the Ag atoms are additionally co-ordinated by two S atoms of the neighboring chains with weak Ag–S interactions (288.6 and 299.7 pm; [2 + 2] co-ordination of the Ag atoms).

Fig. 5 shows that [AgCu(SCN)$_2$(py)$_3$] **6** consists of ten-membered rings which are formed by two Ag$^+$ and two SCN$^-$ ions, one Cu$^+$ ion and one S atom of a further SCN$^-$ unit. These rings are linked by common Ag–S bonds to polymeric strands featuring 1,3-μ- and 1,1,3-μ$_3$-bridging SCN$^-$ ligands. In accordance with the HSAB principle, the "harder" N atoms bind to copper and the "softer" S atoms to silver. The distorted tetrahedral co-ordination of the Cu atoms is completed by two pyridine molecules and that of the Ag atoms by one pyridine ligand.

Compound **6** crystallizes in space group *Fdd*2, with the polymeric chains running parallel to the face diagonals [0 1 1] and [0 1 −1] of the unit cell. According to the space group symmetry, layers of these strands are perpendicular to the [1 0 0] direction. These layers are stacked in such a way that the direction of the AgCu(SCN)$_2$(py)$_3$ chains is turned by ±86.79° from layer to layer as shown in Fig. 5(b).
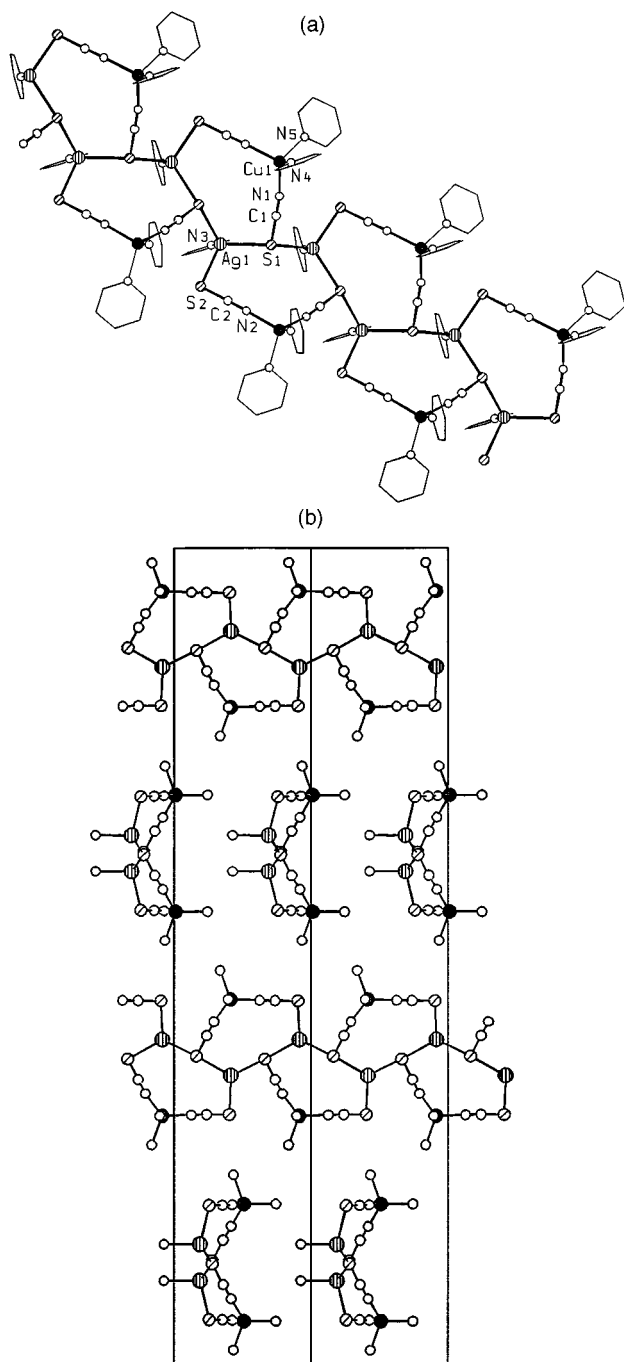
**Fig. 5** Crystal structure of compound **6**: (a) fragment of the polymeric chain, Ag–S1 262.0(2), Ag–S1′ 258.9(2), Ag–S2 255.8(2), Ag–N3 231.4(5), Cu–N1 197.1(6), Cu–N2′ 198.5(7), Cu–N4 205.0(6), Cu–N5 209.1(5), S1–C1 165.9(7), C1–N1 114.9(8), S2–C2 165.3(8) and C2–N2 114.0(8) pm; (b) packing of the AgCu(SCN)₂(py)₃ chains in the unit cell (pyridine ligands are represented by their N atoms only) viewed along [0 1 1].

In [Ag₂Cu(SCN)₃(py)₃] **7** (space group *Pc*†) a two-dimensional Ag₂Cu(SCN)₃ network is formed that expands perpendicular to the crystallographic *a* axis [Fig. 6(a)]. Each SCN⁻ group acts as 1,1,3-μ₃ bridge and links two Ag and one Cu atom. The Ag atoms are co-ordinated by three S atoms with one pyridine ligand to complete the approximately tetrahedral surroundings [S–Ag–S 110.28–115.37(7), S–Ag–N 103.1–112.2(2)°]. Three N atoms of the SCN⁻ units and one pyridine

---

† The Ag₂Cu(SCN)₃ skeleton in compound **7** complies with the symmetry criteria of space group *Am*; only the orientation of the pyridine ligands destroys this symmetry, therefore refinement without disorder is only possible in space group *Pc*. Reflections *hkl* with *k* + *l* = 2*n* + 1 are weak, but not systematically absent.
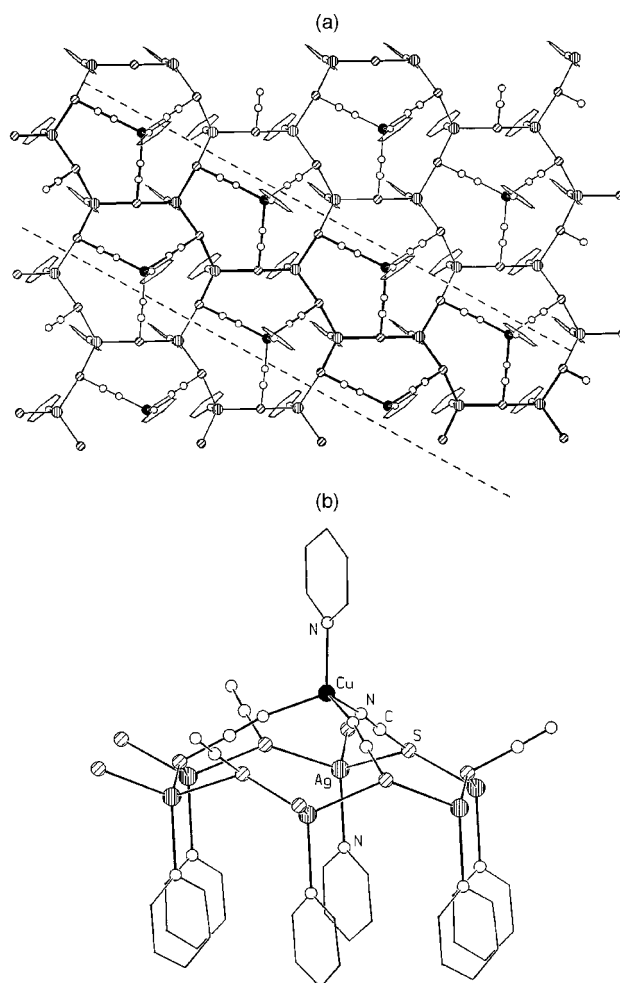
**Fig. 6** Crystal structure of compound **7**: (a) projection of the polymeric network of **7** approximately along [1 0 0]; one AgCu(SCN)₂ chain corresponding to the structure of **6** is highlighted; (b) tent-like fragment showing one Ag₆(SCN)₆ unit capped with a Cu(py) fragment. Selected bond lengths: Ag1–S1 256.6(2), Ag1–S1′ 261.5(2), Ag1–S2 263.3(2), Ag1–N4 231.1(5), Ag2–S2 261.0(2), Ag2–S3 258.3(2), Ag2–S3″ 262.0(2), Ag2–N5 231.2(5), Cu–N1 199.2(5), Cu–N2‴ 198.5(6), Cu–N3 197.4(5), Cu–N6 208.0(6), S1–C1 166.5(6) and C1–N1 114.9(8) pm.

molecule [N–Cu–N 102.3–113.7(2)°] bind to the Cu atoms, also with approximately tetrahedral geometry. Linking of the Ag⁺ ions with the S atoms of the SCN⁻ groups leads to a honeycomb-like net of Ag₆S₆ rings (view along the [1 0 0] direction). Above each of these twelve-membered rings is a Cu(py) fragment that is bound to the N atoms of the SCN⁻ groups. A fragment of the resulting tent-like structure is shown in Fig. 6(b).

Compound **7** also contains ten-membered Ag₂Cu(SCN)₂S rings that have approximately the same shape as the corresponding rings in **6**. Formally **7** may be formed by the condensation of polymeric AgCu(SCN)₂(py)₃ chains in **6** to form the Ag₂Cu(SCN)₃(py)₃ layers, which share common CuSCN edges. One of these chains is outlined in bold in Fig. 6(a). The condensation of two equivalents of **6** to form **7** by splitting off [Cu(SCN)(py)₃] is observed in the experiment: crystals of **6** transform to **7** upon further addition of diethyl ether to the pyridine solution. Single crystals of **7** are obtained after initial formation of **6** from the pyridine–ether solution or from more dilute solutions.

## Conclusion

Ligand stabilized, neutral thiocyanate complexes of monovalent Cu⁺ or Ag⁺ as well as heteronuclear complexes are accessible by use of solvents with distinct donor properties like

**Table 2** Crystallographic data of compounds **1**–**7**

| | **1** | **2** | **3** | **4** | **5** | **6** | **7** |
|---|---|---|---|---|---|---|---|
| Formula | $C_6H_5CuN_2S$ | $C_{11}H_{10}CuN_3S$ | $C_6H_5AgN_2S$ | $C_{11}H_{10}AgN_3S$ | $C_{22}H_{20}AgCuN_6S_3$ | $C_{17}H_{15}AgCuN_5S_2$ | $C_{18}H_{15}Ag_2CuN_6S_3$ |
| $M$ | 200.72 | 279.8 | 245.1 | 324.2 | 604.0 | 524.9 | 690.8 |
| Crystal system | Monoclinic | Monoclinic | Orthorhombic | Orthorhombic | Monoclinic | Orthorhombic | Monoclinic |
| $a$/pm | 1743.5(9) | 585.0(3) | 402.21(5) | 777.2(2) | 1432.50(7) | 5230.5(4) | 898.08(6) |
| $b$/pm | 385.5(2) | 1407.6(6) | 1097.5(1) | 1708.4(4) | 1095.67(5) | 1208.8(1) | 1500.1(1) |
| $c$/pm | 1115.9(6) | 1479.2(8) | 1780.9(2) | 1849.5(4) | 1714.74(7) | 1278.5(1) | 842.19(6) |
| $\beta$/° | 107.55(2) | 94.80(4) | 90 | 90 | 110.686(4) | 90 | 92.288(6) |
| $U$/10⁶ pm | 715.1(6) | 1214(1) | 786.1(2) | 2456(1) | 2517.9(2) | 8084(1) | 1133.7(1) |
| $T$/K | 270 | 200 | 213 | 213 | 213 | 213 | 300 |
| Space group | $Cc$ (no. 9) | $P2_1/n$ (no. 14) | $P2_12_12_1$ (no. 19) | $Pca2_1$ (no. 29) | $P2_1/n$ (no. 14) | $Fdd2$ (no. 43) | $Pc$ (no. 7) |
| $Z$ | 4 | 4 | 4 | 8 | 4 | 16 | 2 |
| $D_c$/g cm⁻³ | 1.864 | 1.531 | 2070 | 1.754 | 1.593 | 1.725 | 2.024 |
| $\mu$(Mo-K$\alpha$)/cm⁻¹ | 3.26 | 1.95 | 2.75 | 1.79 | 1.81 | 2.24 | 2.93 |
| Diffractometer | STOE STADI IV | STOE IPDS | STOE STADI IV | STOE IPDS | STOE STADI IV | STOE STADI IV | STOE STADI IV |
| $2\theta$ range/° | 3.0–56.0 | 9.5–50.0 | 3.0–50.0 | 5.0–54.0 | 3.0–52.0 | 3.0–50.0 | 3.0–56.0 |
| Reflections measured | 1559 | 8267 | 2892 | 12217 | 6953 | 4195 | 5650 |
| Unique reflections ($R_{int}$) | 1551 (0.059) | 2111 (0.052) | 1387 (0.032) | 5221 (0.041) | 4920 (0.027) | 3580 (0.025) | 5448 (0.024) |
| Observed reflections, $I > 2\sigma(I)$ | 1283 | 1796 | 1052 | 4953 | 4182 | 2925 | 4.403 |
| Parameters | 112 | 185 | 91 | 289 | 290 | 235 | 271 |
| $R1$ (observed reflections) | 0.040 | 0.033 | 0.032 | 0.031 | 0.025 | 0.035 | 0.036 |
| $wR2$ (all reflections) | 0.112 | 0.077 | 0.088 | 0.077 | 0.062 | 0.074 | 0.108 |
| Flack parameter $x$ | −0.01(2) | — | 0.0(1) | −0.06(3) | — | 0.00(2) | 0.00(2) |

pyridine. From solutions of CuSCN or AgSCN in pyridine the complexes **1–4** crystallize depending on the crystallization conditions. From solutions of CuSCN and AgSCN the heteronuclear complexes **5–7** can be isolated selectively as crystalline material. Lower temperatures favor the formation of products with a higher number of pyridine ligands.

The crystal structures of compounds **1–7** show some common features: the M–N–C (M = Cu or Ag) and S–C–N groups are approximately linear, while the M–S–C units are bent. This is in agreement with mesomeric structure **A** and sp hybridization of the N atom.

$$^{-}S\text{–}C\equiv N \longleftrightarrow S\text{=}C\text{=}N^{-}$$
$$\textbf{A} \qquad\qquad \textbf{B}$$
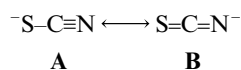
In contrast to sulfur co-ordination, bonding *via* the N atom to a metal ion should favor mesomeric form **B** (sp² hybridized nitrogen)[15] and significant deviations from linearity of the M–N–C group are occasionally observed. In addition steric demands and packing effects may contribute to the arrangement of the SCN⁻ ligand.[18]

The monovalent Cu and Ag atoms of all compounds feature distorted tetrahedral co-ordination geometries and the thiocyanate ligands act as μ or μ₃ bridges. The Ag–S distances (248.4–275.9 pm) vary much more than the Cu–S (230.2–237.7 pm) or the Cu–N (NCS) bond lengths (194.1–199.2 pm). In spite of these common structural features, compounds **1–7** differ in the second and higher co-ordination spheres and show a great structural variety. In the heteronuclear compounds the SCN⁻ ligands co-ordinate to the metal atoms according to Pearson's principle[7] of "hard and soft Lewis acids and bases": the sulfur atom of the thiocyanate ligand favors the larger, "softer" Ag⁺ ions, whereas the "harder" nitrogen atom prefers the smaller Cu⁺ ions. This behavior leads among other things to the structural variations found in **2**, **4** and **5** {[MM′(SCN)₂(py)₄]; M, M′ = Cu or Ag}.

The co-ordination to metal atoms has no significant influence on the geometry of the SCN⁻ groups. The three vibration bands of the thiocyanate ligands in the infrared or Raman spectra are more influenced by the electronic situation and give information about bridging or terminal co-ordination. However, it is not always possible to deduce the mode of bridging definitively from vibrational data. For example the values for the vibrational modes of 1,3-μ bridging SCN⁻ do not differ significantly from those of 1,1,3-μ₃ ligands. However, even knowledge of the co-ordination mode on the basis of vibrational spectra usually does not allow a conclusion to be reached on the long range order.

## Experimental

### Preparations

**[Cu(SCN)(py)] 1.** The compound CuSCN (1.82 g, 15 mmol) was dissolved in pyridine (35 cm³). Addition of diethyl ether (50 cm³) to the slightly green pyridine solution led to the formation of **1** as a white crystalline powder which was filtered off, washed with ether and dried *in vacuo*. Colorless crystals of **1** were obtained by slow addition of ether to the CuSCN solution in pyridine (2.89 g, 96%) (Found: C, 35.95; H, 2.53; N, 13.78. $C_6H_5CuN_2S$ requires C, 35.91; H, 2.51; N, 13.95%) Raman: ṽ/cm⁻¹ = 3063m, 2120vs, 1597m, 1223w, 1155w, 1038w, 1009m, 753w, 650vw, 628w and 448w.

**[Cu(SCN)(py)₂] 2.** The compound CuSCN (0.22 g, 1.8 mmol) was dissolved in pyridine (3 cm³). Slow evaporation of the pyridine at a pressure of 25 mbar (bar = 10⁵ Pa) led to the formation of yellow-green rods of **2** within 3 d (0.30 g, 83%). When separated from the mother-liquor **2** decomposes by loss of pyridine.

Raman: ṽ/cm⁻¹ = 3062m, 2099s, 1593m, 1292w, 1217w, 1034w, 1007s, 767m, 652w, 625 (sh) and 463w.

**[Ag(SCN)(py)] 3 and [Ag(SCN)(py)₂] 4.** The compound AgSCN (83 mg, 0.50 mmol) was dissolved in pyridine (1.5 cm³). Layering the colorless solution with diethyl ether (5 cm³) at room temperature yielded colorless platelets of **3** (90 mg, 73%). Crystals of the same compound were obtained in quantitative yield by slow evaporation of the solvent at reduced pressure at room temperature. Complete evaporation of the solvent caused decomposition by liberation of pyridine (Found: C, 29.00; H, 2.01; N, 11.26. $C_6H_5AgN_2S$ requires C, 29.41; H, 2.06; N, 11.43%); Raman: ṽ/cm⁻¹ = 2116s and 745m. Compound **4** formed as colorless needles upon layering a solution of AgSCN (166 mg, 1.00 mmol) in pyridine (7 cm³) with ether at −30 °C (100 mg, 40%). When separated from the pyridine solution **4** decomposes by rapid loss of pyridine.

**[AgCu(SCN)₂(py)₄] 5.** The compounds CuSCN (61 mg, 0.50 mmol) and AgSCN (83 mg, 0.50 mmol) were dissolved in pyridine (15 cm³). Layering of the yellow solution with diethyl ether (10 cm³) at −30 °C yielded yellow crystals of **5** which decomposes at room temperature or after separating from the pyridine solution (60 mg, 20%).

**[AgCu(SCN)₂(py)₃] 6 and [Ag₂Cu(SCN)₃(py)₃] 7.** The compounds CuSCN (122 mg, 1.0 mmol) and AgSCN (166 mg, 1.0 mmol) were dissolved in pyridine (7 cm³). Slow evaporation of the solvent at reduced pressure (25 mbar) yielded yellow crystals (platelets) of **6** (236 mg, 45%). Crystallization by diluting the pyridine solution with small amounts of diethyl ether initially gave crystals of the same product. However, with increasing concentration of ether the crystals converted into **7**. Pure **7** could be obtained as yellow prismatic crystals by reaction of CuSCN (61 mg, 0.50 mmol) and AgSCN (166 mg, 1.0 mmol) in pyridine (6 cm³) and layering with diethyl ether (10 cm³) (270 mg, 78%) (Found: C, 31.24; H, 2.22; N, 12.08. $C_{18}H_{15}Ag_2Cu$-$N_6S_3$ requires C, 31.35; H, 2.19; N, 12.16%). Raman: ṽ/cm⁻¹ = 2113s, 751m and 448w.

### X-Ray analyses of compounds 1–7

The data collections were performed on STOE STADI IV four circle and STOE IPDS imaging plate diffractometers using Mo-Kα radiation. All intensities were corrected for Lorentz-polarization effects. Empirical absorption corrections were applied for **1**, **3** and **5–7**. The structures were solved by direct methods (SHELXS 86[19]) and refined by full-matrix least squares based on $F^2$ using all measured unique reflections (SHELXL 93[19]). Anisotropic displacement parameters were used for all non-hydrogen atoms. Hydrogen atoms were localized and refined (**1** and **2**) or included in calculated positions (**3–7**). Other important crystallographic data are summarized in Table 2. Graphical presentations were drawn using SCHAKAL 92.[20]

CCDC reference number 186/1092.

See http://www.rsc.org/suppdata/dt/1998/3071/ for crystallographic files in .cif format.

## Acknowledgements

## References

1 H. Krautscheid, *Z. Anorg. Allg. Chem.*, 1995, **621**, 2049; H. Krautscheid and F. Vielsack, *Angew. Chem.*, *Int. Ed. Engl.*, 1995, **34**, 2035; *Z. Anorg. Allg. Chem.*, 1997, **623**, 259.

2   D. L. Smith and V. D. Saunders, *Acta Crystallogr., Sect. B*, 1981, **37**, 1807; 1982, **38**, 907.
3   M. Kabesova, M. Dunaj-Jurco, M. Serator, J. Gazo and J. Garaj, *Inorg. Chim. Acta*, 1976, **17**, 161.
4   J. L. Burmeister, *Coord. Chem. Rev.*, 1966, **1**, 205; 1968, **3**, 225; 1990, **105**, 77.
5   R. A. Bailey, S. L. Kozak, T. W. Michelsen and W. N. Mills, *Coord. Chem. Rev.*, 1971, **6**, 407; A. H. Norbury, *Adv. Inorg. Chem. Radiochem.*, 1975, **17**, 231.
6   M. Kabesova, R. Boca, M. Melnik, D. Valigura and M. Dunaj-Jurco, *Coord. Chem. Rev.*, 1995, **140**, 115.
7   R. G. Pearson, *J. Am. Chem. Soc.*, 1963, **85**, 3533; M. K. Kroeger and R. S. Drago, *J. Am. Chem. Soc.*, 1981, **103**, 3250.
8   K. Vrieze and G. van Koten, in *Comprehensive Coordination Chemistry*, Pergamon, Oxford, 1987, vol. 2, p. 225.
9   G. O. Morpurgo, G. Dessy and V. Fares, *J. Chem. Soc., Dalton Trans.*, 1984, 785; P. C. Healy, B. W. Skelton, A. F. Waters and A. H. White, *Aust. J. Chem.*, 1991, **44**, 1049.
10  N. K. Mills and A. H. White, *J. Chem. Soc., Dalton Trans.*, 1984, 229.
11  P. C. Healy, C. Pakawatchai, R. I. Papasergio, V. A. Patrick and A. H. White, *Inorg. Chem.*, 1984, **23**, 3769.
12  L.-N. Rudolph, Ph.D. Thesis, Freie Universität Berlin, 1996; C. L. Raston, B. Walter and A. H. White, *Aust. J. Chem.*, 1979, **32**, 2757; G. J. Pyrka, Q. Fernando, M. B. Inoue and M. Inoue, *Inorg. Chim. Acta*, 1989, **156**, 257.
13  L.-N. Rudolph and H. Hartl, *Z. Anorg. Allg. Chem.*, 1997, **623**, 687.
14  C. Potvin, J.-M. Manoli, F. Sécheresse and S. Marzak, *Inorg. Chem.*, 1987, **26**, 4370; J.-M. Manoli, C. Potvin, F. Sécheresse and S. Marzak, *Inorg. Chim. Acta*, 1988, **150**, 257.
15  A. Tramer, *J. Chim. Phys. Chim. Biol.*, 1962, **59**, 232; M. Kabesova, J. Kohout and J. Gazo, *Inorg. Chim. Acta*, 1978, **31**, L435.
16  R. H. Toeniskoetter and S. Solomon, *Inorg. Chem.*, 1968, **7**, 617; C. G. Macarovici and R. Micu-Semeniuc, *Rev. Roum. Chim.*, 1969, **14**, 357; B. R. S. Sengar and G. Narain, *Zh. Obshch. Khim.*, 1975, **45**, 339; M. A. S. Goher, *Collect. Czech. Chem. Commun.*, 1977, **42**, 1478.
17  I. Lindqvist, *Acta Crystallogr.*, 1957, **10**, 29.
18  A. F. Wells, *Structural Inorganic Chemistry*, Clarendon Press, Oxford, 5th edn., 1995, p. 936.
19  G. M. Sheldrick, SHELXS 86 and SHELXL 93, Programs for Crystal Structure Determinations, Göttingen, 1986 and 1993.
20  E. Keller, SCHAKAL 92, A Fortran Program for Graphical Representation of Molecular and Crystallographic Models, Universität Freiburg, 1992.